

The Effect of Microstructure on Stress Corrosion Cracking Growth Rates of Low Alloy High Strength Steel Welded Joint

Tongjiao Chu¹, Haichao Cui¹, and Fenggui Lu^{1,*}

¹Shanghai Key Laboratory of Materials Laser Processing and Modification, School of Materials Science and Engineering, Shanghai Jiao Tong University, Shanghai 200240, China

Abstract. The correlation of multi-microstructure and stress corrosion sensitivity based on the low alloy high strength steel welded joint was systematically studied in NaCl solution at the high-temperature. Through comparatively measuring the stress corrosion crack (SCC) rate in the different area of base metal (BM) and weld metal (WM) respectively, the SCC resistance in welded joint was evaluated and analysed. The SCC test indicated that the WM presented a lower crack growth rate (CGR) compared to the BM. The reason for that was mainly ascribed to the columnar of WM that impeded the crack growth in the vertical direction of stress. Meanwhile, the interwoven microstructure of nonparallel ferrite strips and fine acicular ferrite in the WM led to the zigzag propagated path and decreased the CGR.

1 Introduction

Stress corrosion cracking (SCC) of welded joint continues to be a crucial problem for the power industry [1, 2]. Complex microstructure in welded joint increases the difficulty to analysis stress corrosion behaviour. The crack growth rate in components is a common method to evaluate the susceptibility of stress corrosion [3, 4]. Yamazaki et al. [5] reported that the CGR in 40% cold worked Alloy 600 was lower than that in the 20% cold worked Alloy 600. Kim et al. [6] investigated the repairing-layer of nuclear power plant, and indicated that high stress in weld metal increases the sensitivity to SCC. The thermal cycles in multi-layers and multi-passes could severely change the material properties [7, 8], such as microstructure, element segregation, precipitation of grain boundary carbides, thus affected the stress corrosion behaviour in the weld metal. In this work, the stress corrosion cracking tests on the welded joint of low alloy high strength steel were conducted in a chloride solution at high temperature with O₂. The crack growth rates of the base metal (BM) and the weld metal (WM) were measured from the curve graph of crack length vs. time. The crack growth paths of the specimens were observed by using an optical microscope (OM) after SCC tests. The detailed characteristics of microstructure with the crack growth rates were addressed by using scanning electron microscope (SEM).

2 Experimental procedures

2.1. Welded joint preparation

Low alloy high strength steels as BMs are used to fabricate the welded joint investigated in this study. Meanwhile, the narrow gap submerged arc welding (NG-SAW) technique was selected to manufacture the welded joint through the multi-layers and multi-passes processes.

2.2 SCC test

Compact tension (CT) specimens with thickness of 12.5 mm and 5% side grooves on each side were prepared, as shown in Fig. 1. The notch of CT specimens were located in BM and the WM, respectively. SCC crack growth rates were measured using a facility equipped with an autoclave and a direct current potential drop (DCPD) crack length measurement system.

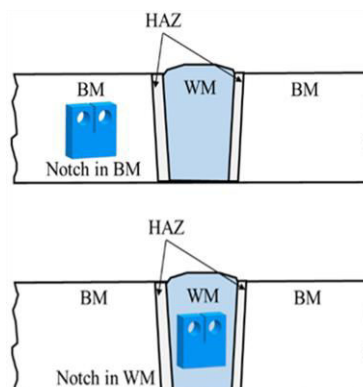


Fig. 1. Method to remove specimens from the welded joint

* Corresponding author: Lfg119@sjtu.edu.cn

2.3 Microstructure characterization

After the stress corrosion cracking test, all the specimens were prepared to microstructure analysis by wire-electrode cutting. Crack growth paths were etched by nital and observed by OM (Zeiss Image A2m), SEM (JSM-7800F) with energy dispersive X-ray spectroscopy (EDS: INCA by Oxford) was used to analysed the detailed characteristics of the crack growth.

3 Results and discussion

In order to better understand the SCC behaviour of the welded joint, microstructure of the welded joint had been observed, as shown in **Fig. 2**. The welded joint was composed by base metal (BM) with temper bainites, heat-affected zone (HAZ) with large size of prior austenite grain (PAG), and weld metal (WM) with fine ferrites. Meanwhile, the WM was divided into columnar grain zone and fine grain zone due to welding thermal cycles. Furthermore, micro-hardness of the welded joint had been measured and shown in **Fig. 3**. It could be found that the hardness of BM was higher than WM, which suggested higher susceptibility in BM.

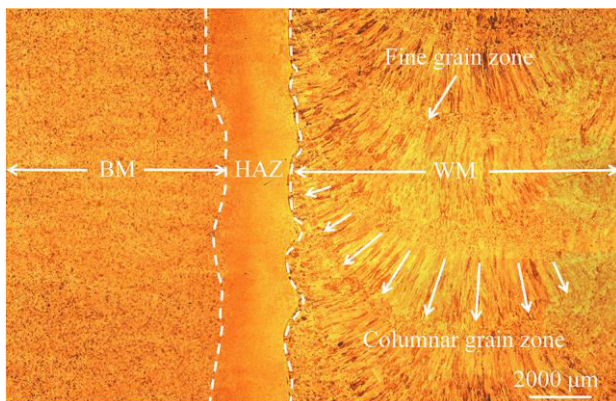


Fig. 2. Optical morphology of the welded joint.

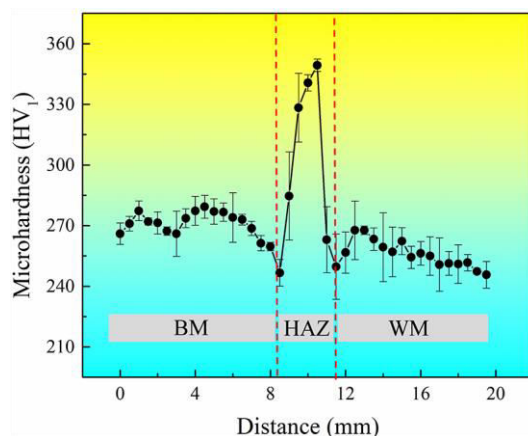


Fig. 3. Micro-hardness of the welded joint.

After the test of stress corrosion cracking, the crack growth rate of the BM and WM are calculated and showed in **Fig. 4**. The same K value of $38 \text{ MPa}\cdot\text{m}^{1/2}$ were carried out on the BM and WM. The BM performed a much higher CGR than the WM, which

agreed well with the prediction from hardness results. The WM has higher crack growth resistance to stress corrosion than the BM, which resulted in the difference of microstructure.

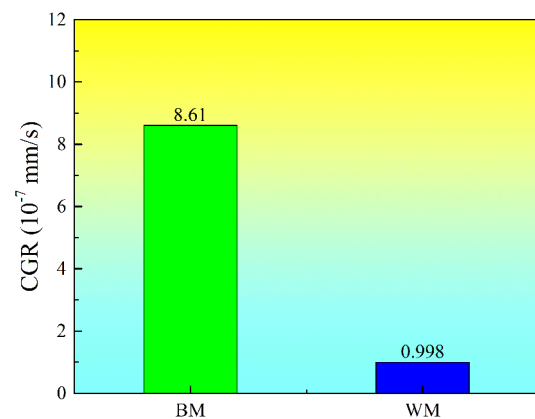


Fig. 4 CGR of the BM and WM in chloride solution at high temperature under same K value.

Crack growth path of the BM is observed by optical microscopy, as shown in **Fig. 5**. The cracks grew through the prior austenite grain boundaries (PAGBs), and presented obvious trans-granular cracking mode. Meanwhile, crack for BM occurred to branch during propagation.

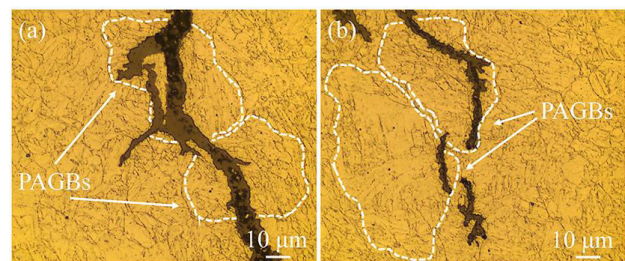


Fig. 5 Optical morphology of the SCC growth path of the BM.

The clear trans-granular cracking mode could be observed in SEM images, as shown in **Fig. 6**. Crack propagated mainly along the lath-martensite, grew in grain boundary occasionally. The Cr-enriched carbide precipitated in the boundary of lath-martensite, which would produce Cr-depleted zone. Thus, the lath-martensite in BM caused lower resistance to SCC.

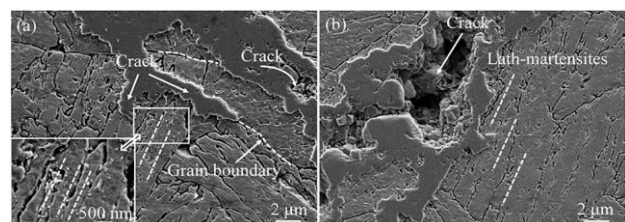


Fig. 6 SEM morphology of the SCC growth path of the BM.

Columnar grain zone and fine grain zone in WM could play significant role in its higher resistance to SCC. As shown in **Fig. 7**, crack occurs to branch when meet columnar zone. This obvious branch could reduce crack growth rate. Then, cracking was inhibited by the

columnar grain, and propagated in slow rate. **Fig. 8** shows the detailed morphology of growth path for the WM. **Fig. 8(a)** clearly displays that the stress corrosion crack growth impedes by the ferrite strips. The acicular ferrites also act as barriers during the crack growth, as shown in **Fig. 8(b)**. Thus, the columnar grain and fine ferrite were the main factor of higher resistance to SCC.

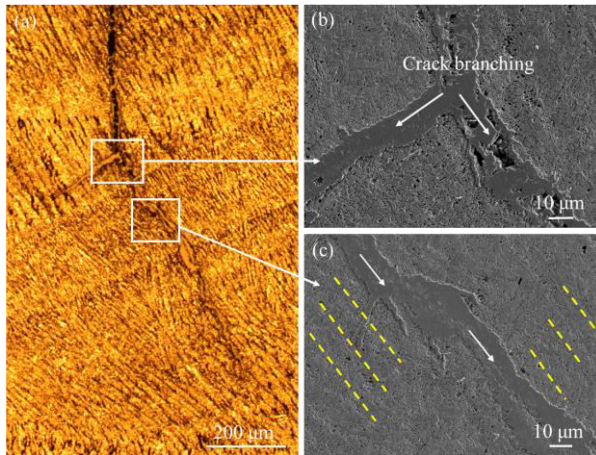


Fig. 7 Morphology of the SCC growth path of the WM.

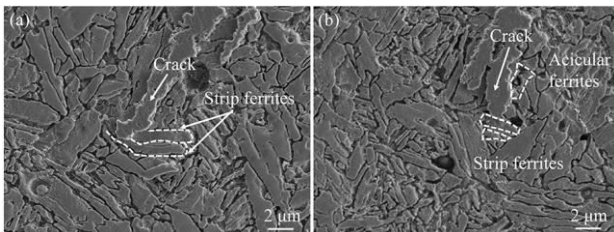


Fig. 8 SEM morphology of the SCC growth path of the WM.

4 Conclusions

SCC tests of the low alloy high strength steel welded joint in chloride solution with O₂ at high temperature were carried out to evaluate susceptibility to stress corrosion cracking. The main conclusions are drawn as following:

1. Under the same K value, the WM remains quite lower CGR and shows a better stress corrosion cracking resistance than BM.
2. The lath-martensites and sub-grain boundary with carbides in prior austenite grain boundary play an important role in acceleration the crack growth for the BM. The interwoven microstructure of nonparallel ferrite strips and fine acicular ferrite in WM generate the tortuous growth path and decrease the CGR.

References

1. B. Roberts, P. Greenfield, *Corros.* **35**, 402 (1979)
2. D.A. Rosario, R. Viswanathan, C.H. Wells, G.J. Licina, *Corros.* **54**, 531 (1998)

3. D.D. Macdonald, P.C. Lu, M. Urquidi-Macdonald, T.K. Yeh, *Corros.* **52**, 768 (1996)
4. T. Cassagne, A. Gelpi, *Proceedings of the sixth international symposium on environmental degradation of materials in nuclear power systems-water reactors* (1993)
5. S. Yamazaki, Z. Lu, Y. Ito, Y. Takeda, T. Shoji, *Corros. Sci.* **50**, 835 (2008)
6. J.D. Kim, C.J. Kim, C.M. Chung, *J. Mater. Process. Technol.* **114**, 51 (2001)
7. J. Sule, S. Ganguly, H. Coules, T. Pirling, *J. Manuf. Process.* **18**, 141 (2015)
8. H. Zhao, G. Zhang, Z. Yin, L. Wu, *J. Mater. Process. Technol.* **212**, 276 (2012)